



## Electrospun collagen–chitosan nanofiber: A biomimetic extracellular matrix for endothelial cell and smooth muscle cell

Z.G. Chen<sup>a,b,\*</sup>, P.W. Wang<sup>a</sup>, B. Wei<sup>c</sup>, X.M. Mo<sup>a,\*</sup>, F.Z. Cui<sup>b</sup>

<sup>a</sup>State Key Laboratory for Modification of Chemical Fibers and Polymer Materials, College of Chemistry, Chemical Engineering and Biotechnology, Donghua University, Shanghai, 201620, China

<sup>b</sup>Department of Materials Science and Engineering, Tsinghua University, Beijing, 100084, China

<sup>c</sup>Shandong Jiaotong University, Jinan 250023, China

### ARTICLE INFO

#### Article history:

Received 8 January 2009

Received in revised form 4 June 2009

Accepted 20 July 2009

Available online 25 July 2009

#### Keywords:

Collagen

Chitosan

Electrospinning

Biomimetic

Biocompatibility

### ABSTRACT

Electrospinning of collagen and chitosan blend solutions in a 1,1,1,3,3,3-hexafluoroisopropanol/trifluoroacetic acid (v/v, 90/10) mixture was investigated for the fabrication of a biocompatible and biomimetic nanostructure scaffold in tissue engineering. The morphology of the electrospun collagen–chitosan nanofibers was observed by scanning electron microscopy (SEM) and stabilized by glutaraldehyde (GTA) vapor via crosslinking. Fourier transform infrared spectra analysis showed that the collagen–chitosan nanofibers do not change significantly, except for enhanced stability after crosslinking by GTA vapor. X-ray diffraction analysis implied that both collagen and chitosan molecular chains could not be crystallized in the course of electrospinning and crosslinking, and gave an amorphous structure in the nanofibers. The thermal behavior and mechanical properties of electrospun collagen–chitosan fibers were also studied by differential scanning calorimetry and tensile testing, respectively. To assay the biocompatibility of electrospun fibers, cellular behavior on the nanofibrous scaffolds was also investigated by SEM and methylthiazol tetrazolium testing. The results show that both endothelial cells and smooth muscle cells proliferate well on or within the nanofiber. The results indicate that a collagen–chitosan nanofiber matrix may be a better candidate for tissue engineering in biomedical applications such as scaffolds.

© 2009 Acta Materialia Inc. Published by Elsevier Ltd. All rights reserved.

### 1. Introduction

Tissue engineering is a recently developed, exciting approach which aims to overcome the limitations of organ transplantation by providing man-made tissues and organs to patients desperately in need of them [1–3]. Its typical method is to incorporate patients' own isolated living cells into three-dimensional polymer scaffolds and to create conditions for cells to proliferate in vitro, then transplant them back to the patient by surgical implantation or in a minimally invasive manner to develop into the desired tissues or organs. The polymer scaffold controls the tissue structure by holding the cells together in a particular three-dimensional structure and by regulating their function as a group. The polymer scaffold also allows the diffusion of nutrients, metabolites and soluble factors, acting as a surrogate for the extracellular matrices (ECM) of tissues in the body

until cells produce an adequate ECM of their own [4]. Such a scaffold, therefore, needs to be developed for in vitro tissue reconstruction as well as for cell-mediated tissue regeneration in vivo.

The challenge of tissue engineering is to create an excellent scaffold. Until now, most of the effort has been focused on developing these polymer scaffolds using biodegradable and biocompatible polymers. An ideal tissue engineering scaffold as a surrogate of the native ECM should mimic the native ECM from both the components and the structure. The native ECM is a molecular complex made up of proteins (especially collagen) and polysaccharides, and comprises three-dimensional hierarchical fibrous structures of nanometer-scale dimensions [5]. Therefore, the scaffold for tissue engineering can be developed by fabricating protein–polysaccharide complex nanofibers.

In native ECM, collagen, as the principal structural elements of the native ECM, exists in a three-dimensional network structure composed of microfibrils on a nanofiber scale. Owing to a wealth of merits such as its biological origin, non-immunogenicity, excellent biocompatibility and biodegradability, collagen has been widely used as biomaterials in the pharmaceutical and medical fields as a carrier for drug delivery [6], dressings for wound healing [7] and tissue engineering scaffold [8]. Chitosan is only a basic nat-

\* Corresponding authors. Address: State Key Laboratory for Modification of Chemical Fibers and Polymer Materials, College of Chemistry, Chemical Engineering and Biotechnology, Donghua University, Shanghai 201620, China. Tel.: +86 010 62773816 (Z.G. Chen).

E-mail addresses: [chenzg2008@163.com](mailto:chenzg2008@163.com) (Z.G. Chen), [xmm@dhvu.edu.cn](mailto:xmm@dhvu.edu.cn) (X.M. Mo).

ural polysaccharide derived from chitin, which is the second natural resource inferior only to the cellulose. Because of its abundant production in nature, excellent biocompatibility, appropriate biodegradability, excellent physicochemical properties and commercial availability at relatively low cost, it has also been widely used as biomaterial in the pharmaceutical and medical fields [9,10].

Chitosan can also form a complex with collagen [11,12], which can cause complementary performance and synergy. Most importantly, chitosan has an analogous structure with glycosaminoglycan, which is the main components of natural ECM. Collagen–chitosan complex is expected to mimic the components of native ECM in designing tissue engineering scaffolds. For many years, the collagen and chitosan blends have also been widely used as biomaterial in pharmaceutical and medical fields [13,14]. They were fabricated into fibers and porous scaffolds on a macroscopic scale by solvent casting [15], wet/dry spinning [16] and freeze drying [17]. However, the native ECM is in the nano-scale fibrous network structure [18]. Recently, it has been found that nanofibrous scaffolds can improve the regeneration of tissues *in vitro*, including bone, cartilage, cardiovascular tissue, nerve and bladder, and minimize scars in regenerated tissues, as human cells can attach and organize well around fibers with diameters smaller than those of the cells [19].

At present, the electrospinning technique has been used as an efficient processing method for manufacturing nanofiber structures for a number of applications [20–22]. A non-woven matrix composed of nanofibers is easily produced via electrospinning, and is architecturally similar to the nanofibrous structure of ECM. Electrospinning of collagen–chitosan complex and their intermolecular interaction have been reported previously [23–25]. But the electrospun collagen–chitosan fiber mesh is not fit for biomimetic extracellular matrix, owing to its sensitivity to water.

In this study, in order to improve the water-resistant property of fibers, electrospun collagen–chitosan complex nanofibers with different chitosan content are crosslinked by glutaraldehyde vapor to mimic the native ECM from both the components and the nanofibrous structure to develop novel biocompatible and biomimetic tissue–engineering scaffolds. The characterization of the biomimetic scaffolds and the cellular activities of endothelial cells (EC) and smooth muscle cells (SMC) on collagen–chitosan bicomponent nanofibrous scaffolds are investigated.

## 2. Materials and methods

### 2.1. Materials

Collagen I (mol. wt.,  $0.8\text{--}1 \times 10^5$  Da) was purchased from Sichuan Ming-rang Bio-Tech Co. Ltd. (China) and chitosan (85%, deacetylated,  $M_n \approx 10^6$ ) was purchased from Ji-nan Hai-de-bei Marine Bioengineering Co. Ltd. (China). Two types of solvents, 1,1,1,3,3,3-hexafluoroisopropanol (HFIP) from Fluorochem Ltd. (UK) and trifluoroacetic acid (TFA) from Sinopharm Chemical Reagent Co., Ltd. (China) were used to dissolve the collagen, chitosan and their blends. A crosslinking agent of aqueous glutaraldehyde (GTA) solution (25%) was purchased from Sinopharm Chemical Reagent Co., Ltd. (China). The porcine iliac artery EC and the myocardial artery SMC of mouse were obtained from Shanghai institutes for biological sciences. All culture media and reagents were purchased from Genom Biomedical Technology Inc. (China).

### 2.2. Electrospinning of collagen and chitosan blend solution

A series of collagen/HFP and chitosan/HFP/TFA solutions were prepared by dissolving collagen and chitosan in HFP and HFP/TFA

mixture, respectively. After the collagen and chitosan were dissolved, the collagen/HFP and chitosan/HFP/TFA solutions were mixed to prepare a series of collagen and chitosan blend solutions (collagen/chitosan = 100/0, 80/20, 50/50, 20/80, 0/100, w/w) at concentrations of 8% ( $\text{g ml}^{-1}$ ) in HFP/TFA mixture (v/v, 90/10). In the electrospinning process, polymer solution was placed into a 5-ml syringe with a needle of inner diameter 0.495 mm. A clamp connected a high voltage power supplier (JDF-1, China) to the needle, and a piece of aluminum foil was placed at  $\sim 130$  mm directly below the needle to act as a grounded collector. The solution formed jets at the tip of the needle, and the jets formed the nanofibers on the grounded collector by the combined force of gravity and electrostatic. The applied voltage and feed rate of the solution were fixed at 16 kV and  $0.8 \text{ ml h}^{-1}$ , respectively. Cover slips with a diameter of 14 mm were also put on the aluminum foil target to collect nanofibers for the biocompatibility investigation. As-spun nanofibers were dried and preserved in a vacuum oven at room temperature.

### 2.3. GTA vapor crosslinking of nanofibers

The crosslinking process was carried out by placing the collagen–chitosan nanofibrous membrane in a sealed desiccator containing 10 ml of 25% glutaraldehyde aqueous solution in a Petri dish. The membranes were placed on a holed ceramic shelf in the desiccator and were crosslinked in an atmosphere of water and glutaraldehyde vapor at room temperature for 2 days. After crosslinking, the samples were exposed in the vacuum oven at normal room temperature.

### 2.4. Nanofiber characterization

The morphology of electrospun collagen–chitosan complex fibers was observed by scanning electron microscopy (SEM) (JSM-5600LV, JEOL, Japan) at an accelerated voltage of 10 or 15 kV. Prior to SEM, the samples were sputter coated with gold. Based on the SEM micrographs, the average diameter and diameter distribution were determined by choosing 100 fibers at random from  $1000\times$  magnification SEM images and analyzing them using image analysis software Adobe Photoshop 7.0, developed by Adobe Systems Inc.

Fourier transform infrared spectroscopy (FTIR) studies were carried out on compressed films containing KBr pellets and samples using a FTIR spectrophotometer (Avatar380, USA). All spectra were recorded in absorption mode at  $2 \text{ cm}^{-1}$  intervals and in the wavelength range  $3800\text{--}600 \text{ cm}^{-1}$ .

The thermal behavior of collagen–chitosan nanofibers was characterized by differential scanning calorimetry (DSC; DSC-822, Mettler-Toledo, Switzerland) in the temperature range  $20\text{--}250 \text{ }^\circ\text{C}$  at a heating rate of  $10 \text{ }^\circ\text{C min}^{-1}$ .

The crystalline structure of the samples was analyzed by X-ray diffraction (XRD) on a wide-angle analyzer (D/max-2500PC, Rigaku) with a  $\text{Cu K}\alpha$  source.

The tensile testing of samples ( $30 \times 10 \text{ mm}^2$ ) was performed using a universal materials tester (H5 K-S, Hounsfield, UK) with a 50 N load cell at ambient temperature  $20 \text{ }^\circ\text{C}$  and humidity 65%. A cross-head speed of  $10 \text{ mm min}^{-1}$  was used for all the specimens tested.

### 2.5. Cell growth and morphology on nanofiber

The nanofibers on cover slips were sterilized with 75% ethanol for 4 h before they were soaked and rinsed five times in phosphate buffer solution (PBS). Thereafter, the nanofibers were soaked in culture medium for 30 min prior to cell seeding in order to facilitate protein adsorption and cell attachment onto the nanofiber surface.

EC and SMC at their third to fourth passages were seeded separately on the nanofibrous membrane, which was held on the bottom of a 24-well tissue culture plate. The seeding density was  $4 \times 10^3$  cells  $\text{cm}^{-2}$  and  $3 \times 10^4$  cells  $\text{cm}^{-2}$ , respectively, in culture medium (DMEM) containing 10% fetal bovine serum and 0.5% penicillin/streptomycin. After a seeding time of 4 h, each culture well was topped up with enough culture medium. The medium was changed every 2 days; the cellular culture was maintained in an incubator at 37 °C with 5%  $\text{CO}_2$ . All experiments were run in triplicate and repeated at least three different times. Cell proliferation on blank tissue culture plates (TCP) served as reference and control substrates.

In order to evaluate cell activity, the cell behavior on nanofibers was monitored for 1, 3, 5 and 7 days or 2, 6, 10 and 14 days ( $n = 3$  for each time point per group) by methylthiazol tetrazolium (MTT) assay. The mechanism behind this assay is that metabolically active cells react with the MTT reagent to produce soluble formazan dye in dimethylsulfoxide, which can be observed at 490 nm. Briefly, the culture medium was removed, and the cultures were washed three times with PBS. About 400  $\mu\text{l}$  serum-free DMEM medium and 40  $\mu\text{l}$  MTT solution were added to each sample, followed by incubation at 37 °C for 4 h to allow the formation of MTT formazan. The medium and MTT were replaced by 400  $\mu\text{l}$  dimethylsulfoxide to dissolve the formazan crystals. After 30 min, the solution was put into 96-well plates, and the samples were read using a microplate reader (MK3, Thermo Electron Corporation, UK) at 490 nm.

SEM was used to examine the morphological characteristics of cells cultured onto the collagen–chitosan complex nanofibrous matrices. After growing for 3 and 6 days, the cellular constructs of the EC and SMC, respectively, were harvested, washed with PBS to remove non-adherent cells and then fixed with 3% glutaraldehyde for 2 h at room temperature, dehydrated through a series of graded alcohol solutions (50%, 70%, 80%, 90%, 95%, 100%), and then air-dried overnight. Dry cellular constructs were sputter coated with gold and observed by SEM at an accelerating voltage of 15 kV.

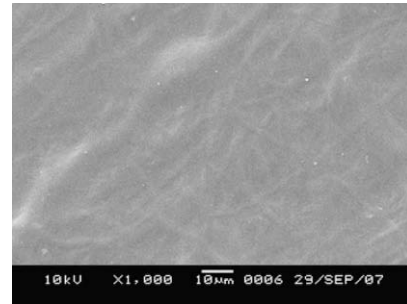


Fig. 2. SEM micrographs of electrospun collagen–chitosan nanofibers with chitosan content of 50% after adding a drop of water.

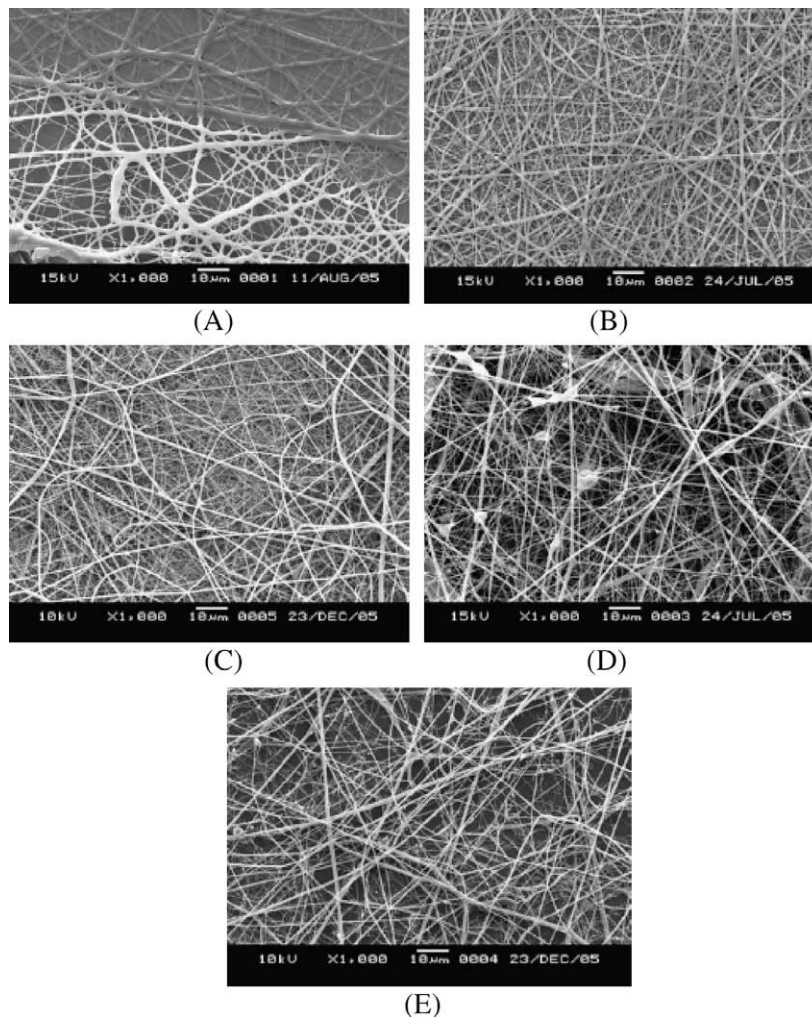
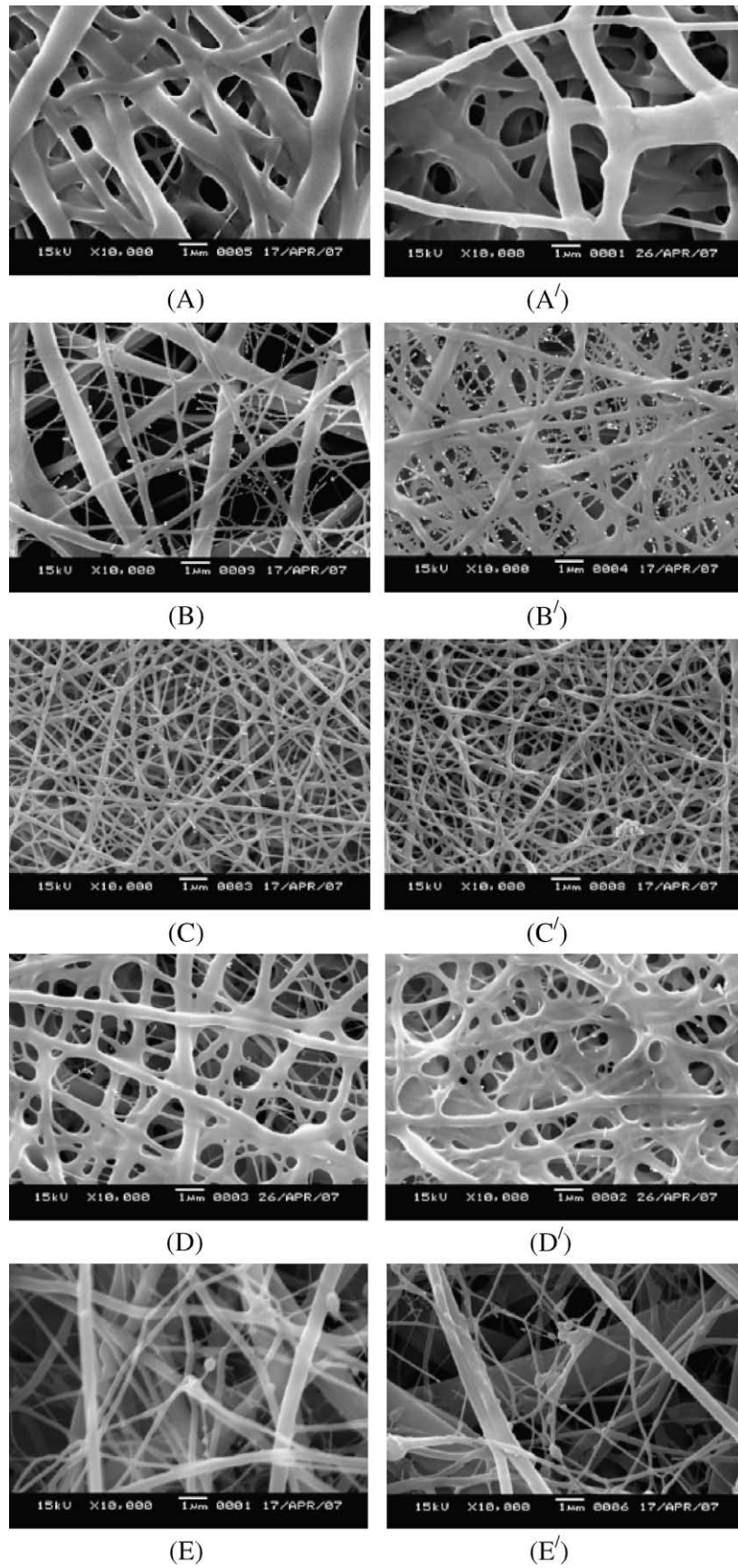


Fig. 1. SEM micrographs of electrospun collagen–chitosan nanofibers with different chitosan content: (A) 0%; (B) 20%; (C) 50%; (D) 80% and (E) 100%.



**Fig. 3.** SEM micrographs of crosslinked collagen–chitosan nanofibers with different chitosan content: (A and A') 0%; (B and B') 20%; (C and C') 50%; (D and D') 80% and (E and E') 100%.

## 2.6. Statistics and data analysis

Cell proliferation of EC and SMC seeded on the collagen–chitosan complex nanofibrous scaffolds were compared by analysis of variance using SPSS 13.0 software. Differences were considered statistically significant for values of  $p < 0.05$ .

## 3. Results and discussion

### 3.1. Morphologies of electrospun collagen–chitosan fibers

Fig. 1 shows SEM micrographs of the electrospun nanofibers composed of collagen and chitosan. Fig. 1A and E shows that pure collagen nanofibers had a higher average diameter ( $810 \pm 580$  nm) than that ( $415 \pm 286$  nm) of pure chitosan nanofibers. The collagen–chitosan complex fibers had different average diameters, with different chitosan content in the fibers. They were  $691 \pm 376$ ,  $515 \pm 253$  and  $434 \pm 263$  nm, with chitosan content of 20%, 50% and 80%, respectively. Fiber diameters decrease with increase in chitosan content. Because applied voltage, collecting distance, solution federate and solution concentration were fixed, fiber diameters are mainly dependent on the ratio of chitosan to collagen. The variety of fiber diameter may be that the organic salt formed between TFA acid and the amino groups on chitosan increase the charge density of the electrospun polymer solution, which results in a higher draw ratio in the electrospinning process [24].

### 3.2. Crosslinking of fibers

Bead-free and randomly arrayed collagen–chitosan nanofibers can be obtained by electrospinning (Fig. 1); however, the nanofibers containing collagen are distensible in water. Even a drop of water on the membranes can immediately destroy the nanofibrous structure, as shown in Fig. 2. Another character is that the electrospun fibers are even able gradually to form point bonds at the fiber junctions if placed in a high humidity ambient. Owing to the sensitivity to water contact or high humidity, the conventional crosslinking approach of immersing samples into aqueous GTA solution is not feasible for crosslinking the present nano-scale collagen–chitosan matrix. By placing the nanofibers into a desiccator filled with GTA vapor, the collagen–chitosan nanofibers can be reasonably crosslinked. Crosslinking of collagen and chitosan with GTA involves the reaction of free amino groups of chitosan and lysine or hydroxylysine amino acid residues of the polypeptide chains with the aldehyde groups of GTA. After GTA vapor crosslinking, the fiber matrix became visibly yellowish and shrunk slightly dimensionally. The color change is due to the establishment of CH=N linkages between the free amine groups of collagen–chitosan and glutaraldehyde [26].

Fig. 3 shows the fiber morphologies of the samples after crosslinked and water-resistant tests. Samples A, B, C, D and E are the collagen–chitosan fibers before the water-resistant test and samples A', B', C', D' and E' are the collagen–chitosan fibers dried for 1 week in a vacuum oven after being immersed in 37 °C water for 4 days. Compared with Fig. 2, the fibrous form was grossly preserved; however, the coexistence of water moisture with GTA vapor during crosslinking treatment had affected the fiber morphology to some extent. This is reflected in the fact that fibers at junctions were fused together, forming bondings (Fig. 3A–E). For the water-resistant test in 37 °C water, the fibrous form of collagen–chitosan was preserved even after 4 days' soaking (Fig. 3A'–E').

### 3.3. FTIR spectroscopy

The IR spectroscopic method has been used frequently to investigate the reaction or intermolecular interaction between two

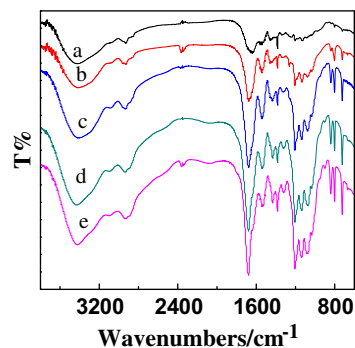


Fig. 4. FTIR spectra of crosslinked electrospun collagen–chitosan complex fibers with different chitosan content: (a) 0%; (b) 20%; (c) 50%; (d) 80% and (e) 100%.

Table 1

Amide absorption bands of crosslinked collagen–chitosan fibers with different chitosan content on FTIR.

	Chitosan content (%)				
	0	20	50	80	100
Amide I ( $\text{cm}^{-1}$ )	1640	1680	1680	1680	1680
Amide II ( $\text{cm}^{-1}$ )	1540	1550	1540	1540	1540
Amide III ( $\text{cm}^{-1}$ )	1240	1260	–	–	–

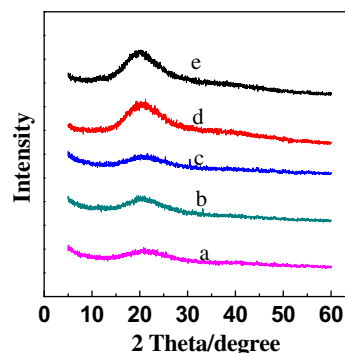


Fig. 5. XRD patterns of crosslinked nanofibers with different chitosan content: (a) 0%; (b) 20%; (c) 50%; (d) 80% and (e) 100%.

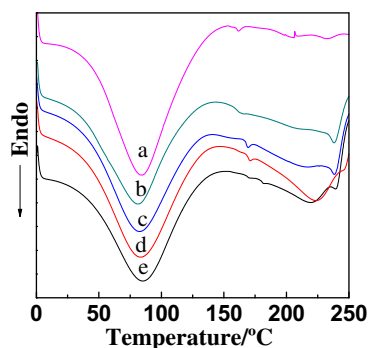
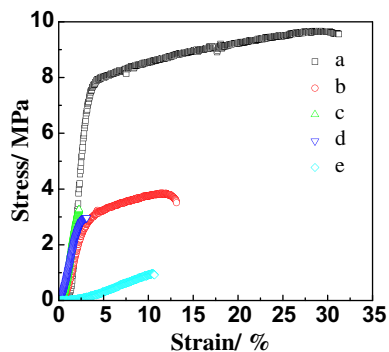


Fig. 6. DSC thermograms of crosslinked collagen–chitosan complex nanofibers with different chitosan content: (a) 0%; (b) 20%; (c) 50%; (d) 80% and (e) 100%.

polymers. The sensitive characteristic absorption bands of collagen and chitosan on the IR spectrum were located in the spectral regions of amide I, amide II and amide III.

FTIR spectra of as-spun collagen–chitosan nanofibers and their interactions were studied in previous work [23,24]. Fig. 4 shows



**Fig. 7.** Typical tensile stress–strain curves of crosslinked collagen–chitosan fibers in dry state with different chitosan content: (a) 0%; (b) 20%; (c) 50%; (d) 80% and (e) 100%.

**Table 2**

Thermal properties of crosslinked collagen–chitosan complex fibers with different chitosan content.

Content of chitosan (%)	0	20	50	80	100
$T_D$ ( $^{\circ}\text{C}$ )	83.9	81.1	82.4	83.2	84.9
$\Delta H_D$ ( $\text{J g}^{-1}$ )	242.3	207.2	180.8	222.6	229.9

FTIR spectra of crosslinked collagen–chitosan nanofibers, and Table 1 gives the amide characteristic absorption bands of crosslinked nanofibers with different chitosan content. Comparing the cross-linked nanofibers with the as-spun nanofibers, the amide absorption bands of crosslinked collagen–chitosan nanofibers did not

change significantly, except that the amide I band of nanofibers with a chitosan content of 20% shifted from 1640 to 1680 and the amide III band of pure collagen fibers disappeared. All this implied that the collagen–chitosan nanofibers did not change significantly, except for enhanced stability after crosslinking by GTA vapor.

### 3.4. XRD analysis

Fig. 5 gives the XRD patterns of crosslinked collagen–chitosan complex nanofibers. The XRD patterns of raw collagen and chitosan were discussed in previous research [25]. After crosslinking, collagen, chitosan and their complex fibers showed a typical amorphous broad peak at  $\sim 20.5^{\circ}$ , which implied that neither collagen nor chitosan molecular chains could be crystallized during electrospinning and crosslinking and give an amorphous structure in nanofibers. The results are similar to the previous research on the as-spun collagen–chitosan fibers. This is due to the cooperative effect of the solvent and electrospinning process on the collagen and chitosan [25].

### 3.5. Thermal behavior

Fig. 6 shows the DSC thermograms of crosslinked collagen–chitosan complex nanofibers. Because collagen and chitosan can be dehydrated or denaturalized when they are heated, the characteristic endothermic peaks in Fig. 6 have often been termed dehydration temperature ( $T_D$ ), and the area of peaks has been termed corresponding endothermic enthalpy ( $\Delta H_D$ ). The values of  $T_D$  and  $\Delta H_D$  are reported in Table 2. Compared with the as-electrospun collagen–chitosan nanofibers reported previously, the crosslinked

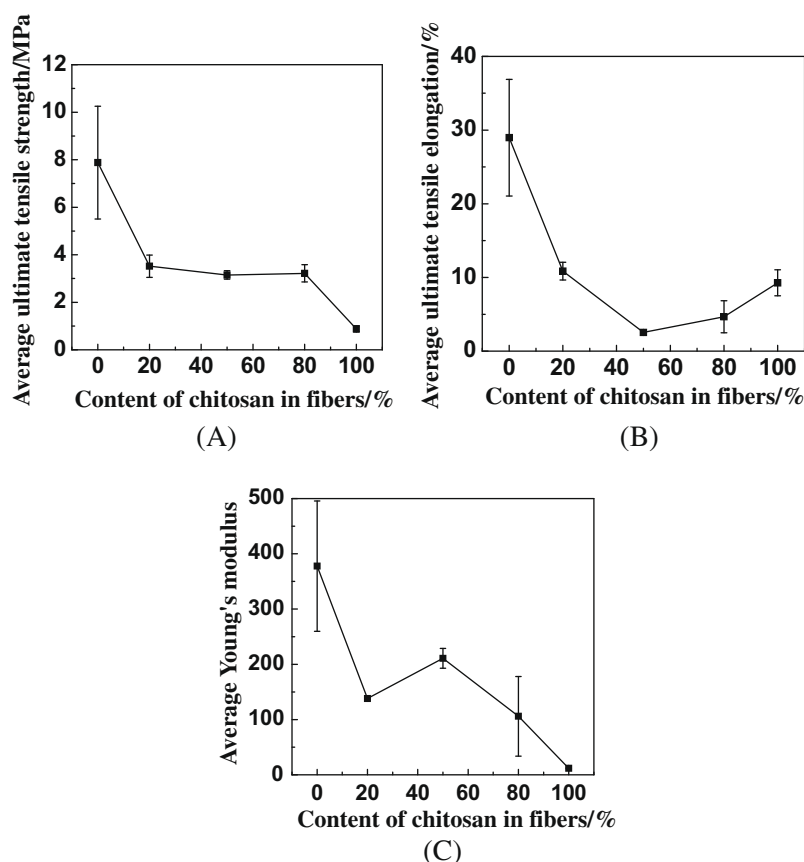


**Fig. 8.** Tensile properties of crosslinked collagen–chitosan complex fibers in dry state. Data are expressed as the mean  $\pm$  SD ( $n = 3$ ).

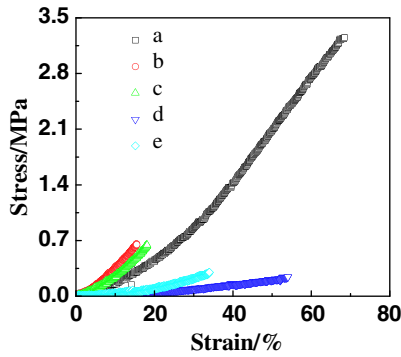


**Fig. 9.** Typical tensile stress–strain curves of crosslinked collagen–chitosan fibers in soaked state with different chitosan content: (a) 0%; (b) 20%; (c) 50%; (d) 80% and (e) 100%.

fibers had higher  $T_D$  and  $\Delta H_D$  [25]. This implies that the electrospun fibers became steadier after crosslinking.

### 3.6. Mechanical properties

The mechanical property of a tissue engineer-scaffold is very important, as it needs to provide an initial biomechanical profile for the cells before new tissue can be formed. Typical tensile stress–strain curves of the crosslinked collagen–chitosan fibrous scaffolds in dry state with different chitosan content are plotted in Fig. 7 for an obvious comparison. Their curve shapes are obviously dissimilar. Based on the stress–strain curves and the further tensile test research, the dependence of the average ultimate tensile strength, the average ultimate tensile elongation and the average Young's modulus of fibrous membrane on chitosan content in the fibers were obtained and are summarized in Fig. 8.

Figs. 7 and 8 clearly show the phenomenon that the nanofibrous membrane resulting from pure collagen exhibits all the largest ultimate tensile strength, the largest tensile modulus and the largest ultimate tensile elongation. In contrast, pure chitosan fiber membrane gave the lowest ultimate tensile strength, the largest tensile modulus and moderate ultimate tensile elongation, whereas the complex collagen–chitosan fiber mats had comparable modulus and strength and showed the lowest ultimate tensile elongation with a chitosan content of 50%. The mechanical properties of fibrous membrane depend on the mechanical properties of the single fibers making up the membrane, the structure of the membrane and the interactions of the fibers making up the mem-

brane. The tensile behavior of collagen–chitosan complex fibers is attributed to the cooperative action of all these factors.

Typical tensile stress–strain curves of the crosslinked collagen–chitosan fiber membrane in soaked state with different chitosan content are also shown in Fig. 9. The fiber mats underwent plastic deformation in the course of stretch, and their stress–strain curve shapes are similar except for the different values of tensile strength and strain at break. Based on the stress–strain curves and further tensile test research, the dependence of the average ultimate tensile strength and the average ultimate tensile elongation of fibrous membrane on chitosan content in the fibers are also summarized in Fig. 10.

From Figs. 9 and 10, the average ultimate tensile strength decreases with the increase in chitosan content in the fibers, whereas the better average ultimate tensile elongation appears in pure collagen fibers and the complex collagen–chitosan fibers with a chitosan content of 80%. In addition to the mechanical properties of single fibers making up the membrane, the structure of membrane and the interactions of fibers making up the membrane, the plasticizing of water also contributes to the tensile behavior of soaked collagen–chitosan complex fibrous membrane.

The average ultimate tensile strength and the average ultimate tensile elongation of the dry and soaked fibrous membrane are summarized in Fig. 11 for an obvious comparison. Compared with the dry fibrous membrane, all the average ultimate tensile strength decreased, whereas all the average ultimate tensile elongation increased to some extent after the fibrous membranes were soaked.

### 3.7. Cell behavior on nanofiber

The biocompatibility of the collagen–chitosan nanofibers scaffold was evaluated *in vitro* by observing and testing the behavior of the third to fourth passage EC and SMC cultured on the fiber scaffold. Cell morphology and the interaction between the cells and nanofibers were studied by SEM. Fig. 12 shows the EC' growth on electrospun collagen–chitosan nanofiber on day 3 after seeding, and Fig. 13 shows the SMC' growth on the same nanofiber on day 6 after seeding. It can be seen that both EC and SMC spread well on the surface of the nanofiber and cells both interact and integrate well with the surrounding fibers. The cells on the nanofibers were also observed to migrate and proliferate in certain patterns and form a continuous monolayer. Most importantly, the SEM images further indicate that the cells on the nanofiber also migrated through the pores into nanofiber mesh and interacted with the surrounding fibers (Fig. 14), which was beneficial for the three-dimensional repair of damaged tissue.

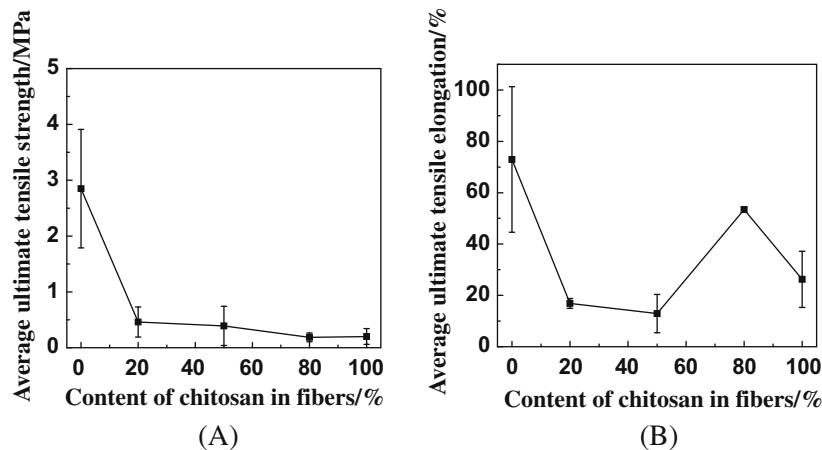


**Fig. 10.** Tensile properties of crosslinked collagen–chitosan complex fibers in soaked state. Data are expressed as the mean  $\pm$  SD ( $n = 3$ ).

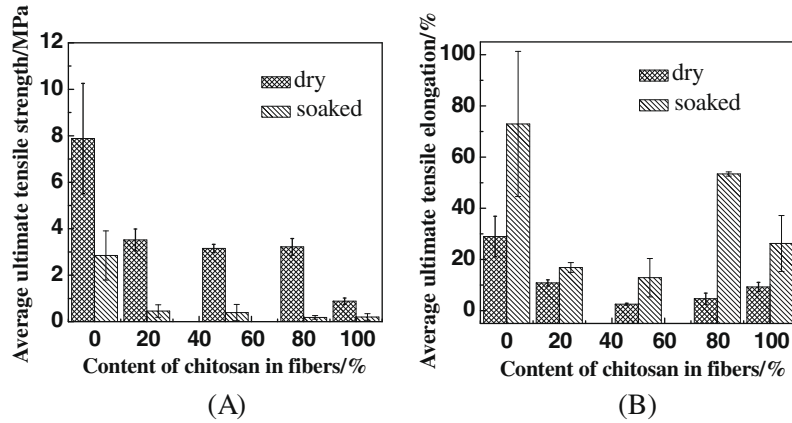


Fig. 11. Comparison of tensile properties of crosslinked collagen–chitosan complex fibers in dry and soaked state.

Cell proliferation on electrospun collagen–chitosan nanofibers was studied *in vitro* by MTT test. Because differences in the chemical composition, conformation, porosity and hydrophilicity of collagen–chitosan nanofibers affect cellular activities [15,27], time-dependent changes were observed in the cellular behavior

in response to collagen–chitosan nanofibrous scaffolds with different blend compositions. In 7-day or 14-day cell cultures, the cell number increased with culture time on all tested groups (Figs. 15 and 16). At the earlier time point (day 1 for EC and day 2 for SMC), the cell numbers on electrospun collagen–chito-

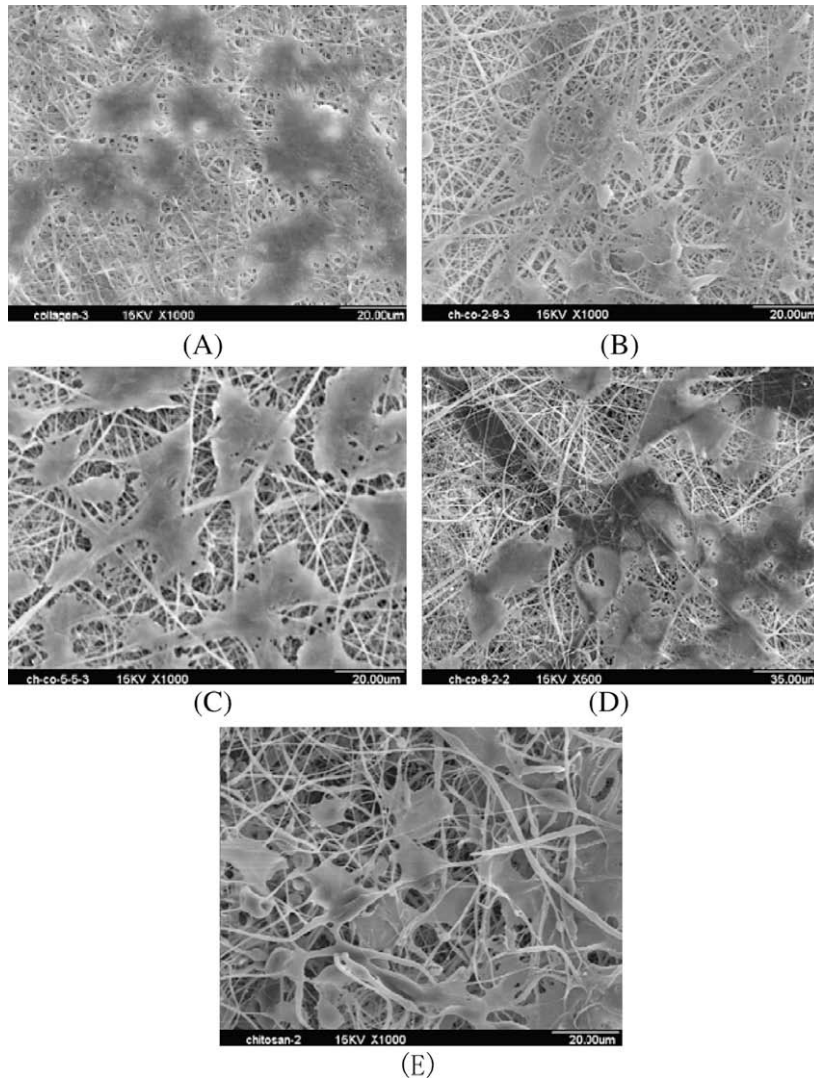
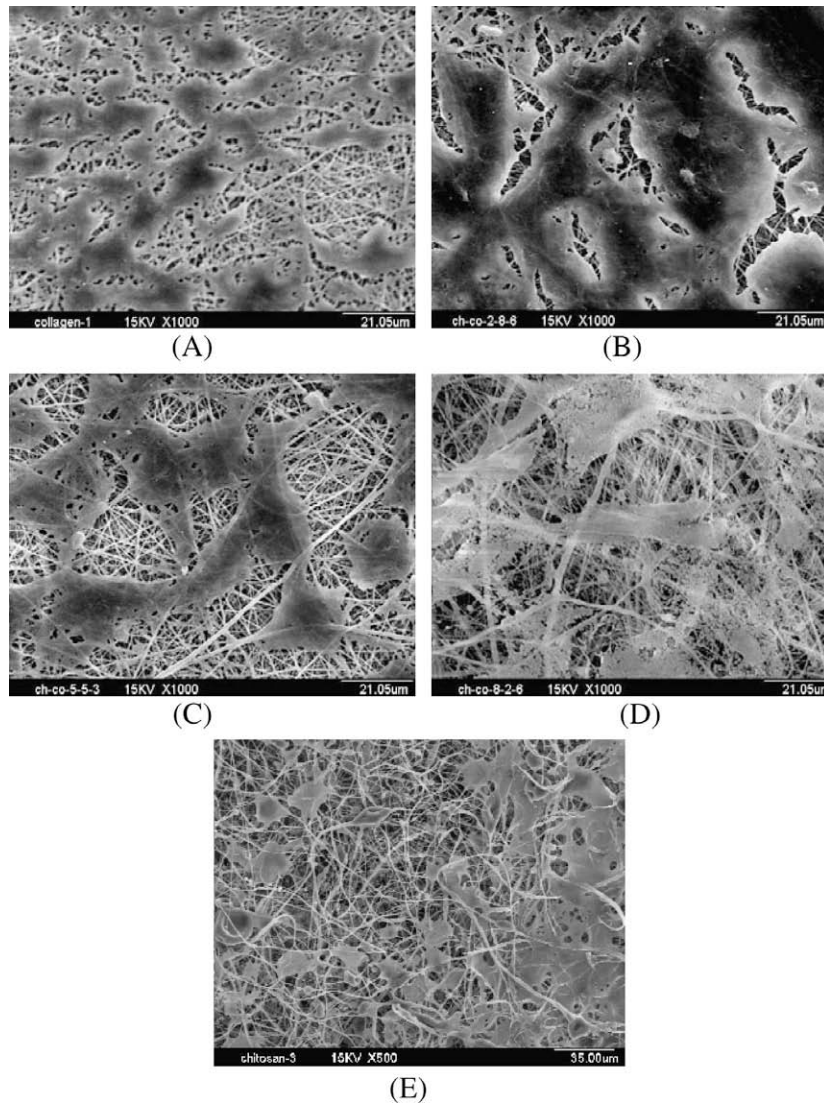
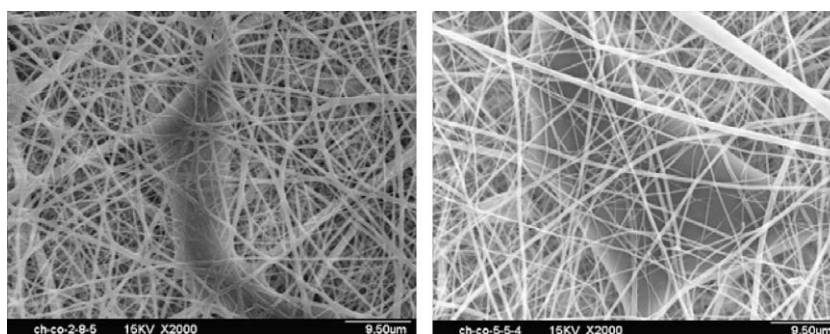


Fig. 12. SEM micrographs of EC seeded on electrospun collagen–chitosan fiber scaffolds with different chitosan content: (A) 0%; (B) 20%; (C) 50%; (D) 80% and (E) 100%.



**Fig. 13.** SEM micrographs of SMC seeded on electrospun collagen–chitosan fiber scaffolds with different chitosan content: (A) 0%; (B) 20%; (C) 50%; (D) 80% and (E) 100%.



**Fig. 14.** SEM micrographs of cells migration into fiber mesh.

san fibrous scaffolds were significantly higher than that on TCP, which implied that the fibrous scaffolds favored cell attachment. When the cell proliferation between the collagen–chitosan nanofiber matrices and TCP were compared, the EC' response on the collagen–chitosan nanofiber matrices with a chitosan content of 50% and pure chitosan fibers did not significantly differ from that on TCP on day 5. Similarly, the SMC' response on collagen–chitosan nanofiber matrices with chitosan content of 20%,

50% and pure chitosan did not differ significantly from that on TCP on day 10. This demonstrated that the nanofiber scaffolds with a chitosan content of 20%, 50% and pure chitosan favored cell proliferation more. Statistical analysis showed that the cells' response between the nanofibers and TCP had a barely significant difference on day 7 for EC and on day 14 for SMC. The reason is that the cell proliferation is inhibited to a certain extent when they proliferate.

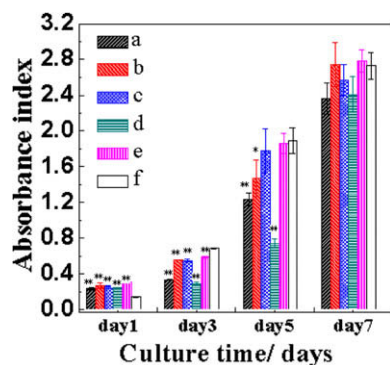


**Fig. 15.** Comparison of EC proliferation on electrospun collagen–chitosan nanofibers with different chitosan content and TCP: (a) 0%; (b) 20%; (c) 50%; (d) 80%; (e) 100% and (f) TCP. Error bars represent mean  $\pm$  SD for  $n = 3$ . \* $p < 0.05$ ; \*\* $p < 0.01$  (compared with EC cultured on TCP at same time point).

In the above experiments on EC and SMC' behavior on electrospun collagen–chitosan nanofiber scaffold, it was found that the protein–polysaccharide bicomponent nanofibers and this novel structure with a high surface area-to-volume ratio and porosity favors cell attachment and proliferation by providing a component and a three-dimensional extracellular environment similar to that of native tissue, as well as a high level of surface area and porosity. The cells not only interact well with the fibers, but also proliferate well on the scaffold, indicating a biological function of the cells within the scaffold. Although the reason for the excellent cell attachment and proliferation on the collagen–chitosan scaffolds remains unclear, it may be a consequence of the formation of particular and proper environments. A proper environment includes proper components and conformation, various nanofiber diameters and high porosity for cell attachment and growth as well as the maintenance of good biological properties with both collagen and chitosan by electrospinning. In addition, one cannot rule out unexpected molecular interactions caused by mixing collagen and chitosan solutions for the fabrication of collagen–chitosan nanofibrous matrices in the electrospinning process.

Unquestionably, collagen is one of the most promising biomimetic materials, though there is controversy that collagen could have changed into gelatin in HFIP [28]. Further insights into the effect of electrospun nanofibrous matrices composed of different combinations of natural polymers (fibrous proteins and polysaccharides) on cellular responses will increase understanding of scaffold design for tissue engineering.

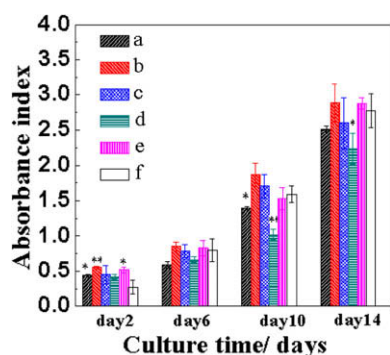


**Fig. 16.** Comparison of SMC proliferation on electrospun collagen–chitosan nanofibers with different chitosan content and TCP: (a) 0%; (b) 20%; (c) 50%; (d) 80%; (e) 100% and (f) TCP. Error bars represent means  $\pm$  SD for  $n = 3$ . \* $p < 0.05$ ; \*\* $p < 0.01$  (compared with SMC cultured on TCP at same time point).

The final goal of scaffold design is to produce an ideal structure that acts as an ECM until host cells can repopulate and resynthesize a new natural matrix. Electrospun collagen–chitosan nanofibrous matrices, especially with a chitosan content of 20%, 50% and pure chitosan, are better potential candidates for cell attachment and proliferation of EC and SMC, which would be especially useful for tissue regeneration. Further application studies of electrospun collagen and chitosan complex fibers will be focused on developing tissue engineering scaffold for the repair and regeneration of blood vessel and nerve tissue.

#### 4. Conclusions

To mimic natural ECM, collagen–chitosan complex nanofibrous scaffolds were obtained by electrospinning, and produced an average fiber diameter in the range 434–691 nm, whereas electrospinning of pure collagen and chitosan produced an average fiber diameter of 810 nm and 415 nm, respectively. GTA vapor was found to be useful for stabilizing the morphologies of electrospun collagen–chitosan fiber. FTIR spectra analysis showed that the collagen–chitosan nanofibers do not change significantly, except for enhanced stability after crosslinking by GTA vapor. XRD analysis implied that both collagen and chitosan molecular chains could not be crystallized in the course of electrospinning and crosslinking, and gave amorphous structure in nanofibers. The thermal behavior and mechanical properties of electrospun collagen–chitosan fibers were also studied by DSC and tensile testing, respectively. The results of cell behavior on nanofiber scaffolds showed that both EC and SMC proliferated well on or within the nanofiber. These results strongly support that the collagen–chitosan nanofibrous matrices, especially with a chitosan content of 20% or 50%, have the advantages of similar components and the nanometer-scale architecture of ECM. They can be beneficial to the damaged tissue repair. Further studies will be focused on developing tissue engineering scaffold for the repair and regeneration of blood vessel and nerve tissue.

#### Acknowledgements

This research was supported by National Nature Science Foundation of China under Grant 30570503, National High Technology Research and Developed Program of China under Grant 2008AA03Z305, Shanghai Sci. and Tech Committee of China under Grants 08520704600 and 0852 381nm03400.

#### Appendix A. Figures with essential color discrimination

Certain figure in this article, particularly Figures 4–7, 9, 15, 16, are difficult to interpret in black and white. The full color images can be found in the on-line version, at [doi:10.1016/j.actbio.2009.07.024](https://doi.org/10.1016/j.actbio.2009.07.024).

#### References

- [1] Mooney DJ, Mikos AG. Growing new organs. *Sci Am* 1999;280:60–5.
- [2] Griffith LG, Naughton G. Tissue engineering—Current challenges and expanding opportunities. *Science* 2002;295:1009–14.
- [3] Langer R, Vacanti JP. Tissue engineering. *Science* 1993;260:920–6.
- [4] Lutolf MP, Hubbell JA. Synthetic biomaterials as instructive extracellular microenvironments for morphogenesis in tissue engineering. *Nat Biotechnol* 2005;23:47–55.
- [5] Nalwa HS. Handbook of nanostructured biomaterials and their applications in nanobiotechnology. Stevenson Ranch, CA: American Scientific Publishers; 2005.
- [6] Prabu P, Dharmaraj N, Aryal S, Lee BM, Ramesh V, Kim HY. Preparation and drug release activity of scaffolds containing collagen and poly (caprolactone). *J Biomed Mater Res A* 2006;79:153–8.

- [7] Gomathi K, Gopinath D, Ahmed MR, Jayakumar R. Quercetin incorporated collagen matrices for dermal wound healing processes in rat. *Biomaterials* 2003;24:2767–72.
- [8] Matthews JA, Wnek GE, Simpson DG, Bowlin GL. Electrospinning of collagen nanofibers. *Biomacromolecules* 2002;3:232–8.
- [9] Adekogbe I, Ghanem A. Fabrication and characterization of DTBP-crosslinked chitosan scaffolds for skin tissue engineering. *Biomaterials* 2005;26:7241–50.
- [10] Huang ZL, Jiang GJ. Manufacture of gelatin/chitosan wound dressing and experimental study on its biological evaluation. *Tissue Eng* 2006;12:1070–1.
- [11] Mo XM. The study of chitosan and gelatin complex. *Acta Polym Sin* 1997;46:222–6.
- [12] Sionkowska A, Wisniewski M, Skopinska J, Kennedy CJ, Wess TJ. Molecular interactions in collagen and chitosan blends. *Biomaterials* 2004;25:795–801.
- [13] Ma L, Gao CY, Mao ZW, Zhou J, Shen JC, Hu XQ, et al. Collagen/chitosan porous scaffolds with improved biostability for skin tissue engineering. *Biomaterials* 2003;24:4833–41.
- [14] Chen RN, Wang GM, Chen CH, Ho HO, Sheu MT. Development of N,O-(carboxymethyl)chitosan/collagen matrixes as a wound dressing. *Biomacromolecules* 2006;7:1058–64.
- [15] Wang XH, Li DP, Wang WJ, Feng QL, Cui FZ, Xu YX, et al. Crosslinked collagen/chitosan matrix for artificial livers. *Biomaterials* 2003;24:3213–20.
- [16] Hirano S, Zhang M, Nakagawa M, Miyata T. Wet spun chitosan-collagen fibers, their chemical N-modifications, and blood compatibility. *Biomaterials* 2000;21:997–1003.
- [17] Lee SB, Kim YH, Chong MS, Lee YM. Preparation and characteristics of hybrid scaffolds composed of beta-chitin and collagen. *Biomaterials* 2004;25:2309–17.
- [18] Silver FH, Christiansen DL. *Biomaterials science and biocompatibility*. New York: Springer; 1999.
- [19] Webster TJ, Waid MC, McKenzie JL, Price RL, Ejirofor JU. Nano-biotechnology: carbon nanofibres as improved neural and orthopaedic implants. *Nanotechnology* 2004;15:48–54.
- [20] Reneker DH, Yarin AL, Fong H, Koombhongse S. Bending instability of electrically charged liquid jets of polymer solutions in electrospinning. *J Appl Phys* 2000;87:4531–47.
- [21] Yarin AL, Koombhongse S, Reneker DH. Bending instability in electrospinning of nanofibers. *J Appl Phys* 2001;89:3018–26.
- [22] Huang ZM, Zhang YZ, Kotaki M, Ramakrishna S. A review on polymer nanofibers by electrospinning and their applications in nanocomposites. *Compos Sci Technol* 2003;63:2223–53.
- [23] Chen ZG, Mo XM, Qing FL. Electrospinning of chitosan collagen complex: to mimic the native extracellular matrix. *Tissue Eng* 2006;12:1074.
- [24] Chen ZG, Mo XM, Qing FL. Electrospinning of collagen–chitosan complex. *Mater Lett* 2007;61:3490–4.
- [25] Chen ZG, Mo XM, He CL, Wang HS. Intermolecular interactions in electrospun collagen–chitosan complex nanofibers. *Carbohydr Polym* 2008;72:410–8.
- [26] Zhang YZ, Venugopal J, Huang ZM, Lim CT, Ramakrishna S. Crosslinking of the electrospun gelatin nanofibers. *Polymer* 2006;47:2911–7.
- [27] Yeo IS, Oh JE, Jeong L, Lee TS, Lee SJ, Park WH, et al. Collagen-based biomimetic nanofibrous scaffolds: preparation and characterization of collagen/silk fibroin bicomponent nanofibrous structures. *Biomacromolecules* 2008;9:1106–16.
- [28] Zeugolis DI, Khew ST, Yew ESY, Ekaputra AK, Tong YW, Yung LYL, Huttmacher DW, Sheppard C, Raghunath M. Electro-spinning of pure collagen nano-fibres—just an expensive way to make gelatin. *Biomaterials* 2008;29:2293–305.